First detection of the visible Mars aurora

J.-C. Gérard[1], S. Aoki[1,2], L. Gkouvelis[1,3], L. Soret[1], Y. Willame[2], I.R. Thomas[2], C. Depiesse[2] B. Ristic[2], A.C. Vandaele[2], B. Hubert[1], F. Daerden[2], M.R. Patel[4], J.-J. López-Moreno[5], G. Bellucci[6], J.P. Mason[4], M.A. López-Valverde[5]

[1]LPAP, STAR Institute, Université de Liège, Belgium

[2]Royal Belgian Institute for Space Aeronomy, Brussels, Belgium

[3]NASA/Ames Research Center, Moffet Field, Mountain view, CA, USA

[4]School of Physical Sciences, The Open University, Milton Keynes, UK

[5]Instituto de Astrofisica de Andalucía/CSIC, Granada, Spain

[6]Istituto di Astrofisica e Planetologia Spaziali, INAF, Rome, Italy

3678 words, 1 table, 3 fig.= 11.4 (/12) print units

30 October 2021

Abstract

We report the detection of nightside visible auroral emission in the Martian aurora based on limb measurements made with the Ultraviolet and VISible spectrometer (UVIS) on board the Trace gas Orbiter. The OI 557.7 nm sporadic emission is mainly localized in the region of strong crustal field of the southern hemisphere, in agreement with ultraviolet auroral observations. The intensity occasionally exceeds 10 kilorayleighs, which makes it detectable with the naked eye of future Mars astronauts. No other visible emission was detected above the sensitivity UVIS threshold. The concentration in the crustal field region and the green line brightness are compatible with earlier ultraviolet observations made from the Mars Express and MAVEN orbiters.

1. INTRODUCTION

The presence of aurora on the Mars nightside was discovered by Bertaux et al. (2005) as the SPectroscopy for the Investigation of the Characteristics of the Atmosphere of Mars (SPICAM) instrument on board the Mars Express orbiter was observing the nightside limb. Prominent spectral features included the CO Cameron bands between 190 and 270 nm and the CO_2^+ ultraviolet doublet (UVD) at 289 nm. Weaker emissions were also detected such as the Fourth Positive CO bands, the [OI] forbidden emission at 297.2 nm and the OI 130.4 nm triplet. This detection lasted a few seconds, indicating that this auroral feature was localized and confined in latitude. This type of aurora was later named discrete aurora in the literature. Leblanc et al. (2008) identified additional ultraviolet auroral events with SPICAM, both in the limb and nadir modes. They showed that the detections were located in regions of statistically open magnetic field lines at 400 km altitude derived by Brain et al. (2007) from measurements by Mars Global Surveyor through electron pitch angle distribution. Gérard et al. (2015) reexamined the SPICAM nadir observations and described 16 discrete aurorae, all located in the southern hemisphere in a region of strong crustal magnetic field. These observations also confirmed that the Mars discrete aurorae are located in magnetic cusp-like structures in the southern hemisphere. Soret et al. (2015) described the characteristics of three limb detections. They determined that the altitude of the ultraviolet emissions was 137 ± 27 km. They also confirmed that the Mars discrete auroral events are located in magnetic cusp-like structures in the southern hemisphere and determined that their latitudinal extent had a mean value of 44 km. The oxygen emission at 297.2 nm was found quite variable, with limb intensities ranging from 98 R to 777 R and a mean value of 360 R. The CO Cameron/O (297.2 nm) ratios ranged from 1.8 to 16.1. Concurrent measurements of the flux of precipitated electrons with the ASPERA-3 instrument confirmed the association between the flux enhancements and the auroral detections, although the aurora was not necessarily observed at the nadir of the MEX spacecraft.

Two types of Martian aurora were later discovered with the Imaging UltraViolet Spectrograph (IUVS) instrument on board the Mars Atmosphere and Volatile EvolutioN (MAVEN) orbiter. The diffuse aurora covers a substantial fraction of the planet' nightside (Schneider et al., 2015). Its presence is linked to the impact of solar energetic particle events as observed during the September 2017 event (Schneider et al., 2018).

Finally, Lyman-α signatures of the dayside proton aurora at low altitude were detected with IUVS (Deighan et al., 2018). Ritter et al. (2018) analyzed the SPICAM database and found that they are triggered by coronal mass ejections and corotating interaction regions. Contrary to discrete and diffuse aurorae, proton aurorae occur on the dayside. They are caused by the direct interaction of the solar wind protons with the Martian corona followed by the interaction of energetic protons and hydrogen energetic neutral atoms with the Martian atmosphere.

Two recent companion papers (Schneider et al., 2021; Soret et al., 2021) based on 6 years of nightside limb observations from the MAVEN orbiter identified 278 occurrences of discrete aurora on Mars. They confirmed earlier results observations showing that frequency and intensity of discrete aurorae are highly correlated with the local crustal magnetic field intensity in the southern hemisphere. They also found that events can also occur in regions of weak or absent crustal fields. They found that events are generally triggered in evening hours, especially under favorable orientations of the interplanetary magnetic field (negative *By*), and may last for hours. Limb profiles of the CO Cameron bands and CO_2^+ UVD showed a peak brightness at 130 ±2.5 km and equal altitude of the two emissions in and out of the region of crustal field. Limb profiles of the [OI] line at 297.2 nm measured peak brightness near 130 km reach up to 0.4 kilorayleighs (one kR corresponds to a surface brightness of 10^9 photons cm^{-2} s^{-1} in 4π steradians) in the valleys of the crustal magnetic field lines with a mean brightness of 0.14 kR. The OI visible green line at 557.7 nm and the UV 297.2 nm emission have a common upper O(1S) excited state with a I(557.7 nm)/I(297.2 nm) ratio of about 16 (Kramida et al., 2019; Gérard et al., 2020). On this basis, Soret et al. (2021) suggested that the oxygen green line brightness may reach a few kilorayleighs. These observations indicated that a green aurora may be observable near 130 km by astronauts in orbit or on the Martian surface at night. They prompted a search for visible aurora with the Ultraviolet and VISible spectrometer (UVIS) instrument on board ESA's Trace Gas Orbiter satellite orbiting Mars.

In section 2, we briefly discuss the UVIS instrument and the special limb observing mode used for the auroral search. Section 3 presents the location and geometry of the observations. The detection and characteristics of the oxygen emission detections are discussed in section 4 as well as with the relation with the characteristics of the

ultraviolet aurora. Finally, section 5 discusses the conditions of observability of the visible aurora during future missions to Mars.

2. THE UVIS-NOMAD INSTRUMENT AND EARLIER DAYGLOW OBSERVATIONS

The UVIS channel (Vandaele, et al., 2015; Patel et al., 2017) is part of the Nadir and Occultation for MArs Discovery (NOMAD) suite of spectrometers designed to perform solar occultations and observe the solar radiation backscattered by the atmosphere (Vandaele et al., 2018). It was flown on board the TGO spacecraft that has been orbiting Mars on a circular orbit at ~400 km altitude inclined 74° to the equator since October 2016. It covers the 200-650 nm spectral range, with a spectral resolution increasing from about 1.2 nm at 200 nm to 1.6 nm at 650 nm. It includes two telescopes, one for solar occultation measurements and a second one for nadir observations of the solar backscattered radiation. The light from the sun or the nadir direction is sent through optic fibers to a plane grating and a collimating mirror on the 1024x256 pixel CCD detector. The photons of the 'nadir' channel travel to the spectrometer through a bundle of optic fiber cables. The nominal integration time is 15 seconds used for the observations reported here. The sensitivity of the instrument is equal to 0.92 count/mW cm^{-2} nm^{-1} sr^{-1}. The field of view is a 43-arcmin circle, which subtends an altitude range of ~8 km at the tangent point from 400 km.

The primary scientific objective of the UVIS nadir channel is to determine the horizontal distribution of atmospheric ozone from the spectral composition of the near ultraviolet solar radiation backscattered by the atmosphere. However, a special observing mode has been designed to investigate the day and night airglows in the upper atmosphere (López-Valverde et al., 2018). During these observations, the TGO spacecraft is slewed in such a way to orient the boresight of the 'nadir' channel toward the limb of the upper atmosphere, away for the direction of the sun. In this observing mode, the altitude resolution at the tangent point depends on the altitude of the spacecraft, the field of view of the instrument and the integration time. The spectra used in this study were integrated over 15 s. The combination of the view angle and the spacecraft motion yields a vertical resolution of 10±5 km at the tangent point.

This special observing mode made it possible to first detect the visible oxygen dayglow at 557.7 nm (Gérard et al., 2020) showing emission peaks near 80 and 120 km

respectively and the red line at 630 nm (Gérard et al., 2021). We now describe the conditions and specificities of the set of nightside observations.

3. THE NIGHTSIDE OBSERVATIONS

During the campaign of nightside observations, a new limb pointing procedure was applied. In this mode, the UVIS line of sight is constrained to keep a quasi-fixed preset tangent altitude during a large fraction of the observations ('limb tracking mode') so that a latitudinal scan is performed. Actually, the tangent altitude usually stabilizes within ~20 km during the course of an observation sequence. For the search for visible auroral signature in the limb-tracking mode, several additional constraints were imposed. The solar zenith angle at the tangent point was larger than 115°. Finally, the altitude of the tangent point was kept nearly constant during the limb tracking phases. 12 orbits of nightside limb profiles have also been collected in the inertial pointing mode, most of them crossing the 130-km region in the crustal field region. In particular, 4 limb-tracking sequences were specifically devoted to the search of visible auroral signature in July 2021. First, the tangent altitude was kept close to 130 km. This altitude statistically corresponds to the mode in the distribution of the peak altitudes of the ultraviolet auroral seen by MAVEN-IUVS. Second, the observations were preferably concentrated in a region of strong crustal magnetic field between 0° and 70° south latitudes and from 110° to 240° longitude. These limits were defined on the basis of the locations of the auroral events observed from Mars Express (Gérard, 2014; Soret, 2015, 2021) and MAVEN (Schneider et al., 2021). Finally, the UVIS field of view was kept oriented as close to East-West (or West-East) when compatible with the spacecraft operational constraints. We note that, at this point, no detection of nightglow emission has been made, even after co-addition of all nightside spectra.

4. THE AURORAL GREEN LINE DETECTION

As expected from the low frequency of the measurable signatures of the ultraviolet aurora (Schneider et al., 2021), individual 15-s spectra rarely show identifiable green line signature. However, Figure 1 shows one of the nightside spectra illustrating a detection of the OI 557.7 nm emission. Three examples of visual identifications of the 557.7 nm feature zoomed on this spectral region are shown in Figure 2. The maps on the right show the locations of the tangent point and the TGO spacecraft during the

observations superimposed on a false-color map indicating the probability of magnetic closed field at 400 km (Brain et al., 2007). The dates, solar zenith angle at the tangent point, spacecraft and tangent point locations and intensities are listed in Table 1. Example (a) was observed outside the strong field rectangle defined earlier but close to the statistical limit between open and closed field line. In example (b), the 557.7 nm signature is located in a 'magnetic valley' where ultraviolet auroral emissions concentrate in Schneider et al. 's (2021) study. Case (c), the strongest of the 3 detections is a zoom on a segment of Figure 1. The tangent point is again located close to the open-closed field boundary. The intensity of the oxygen line is 11 kR. The combination of the 557.7 nm intensity and the sensitivity curve of the UVIS instrument clearly favor the observability of the oxygen green line.

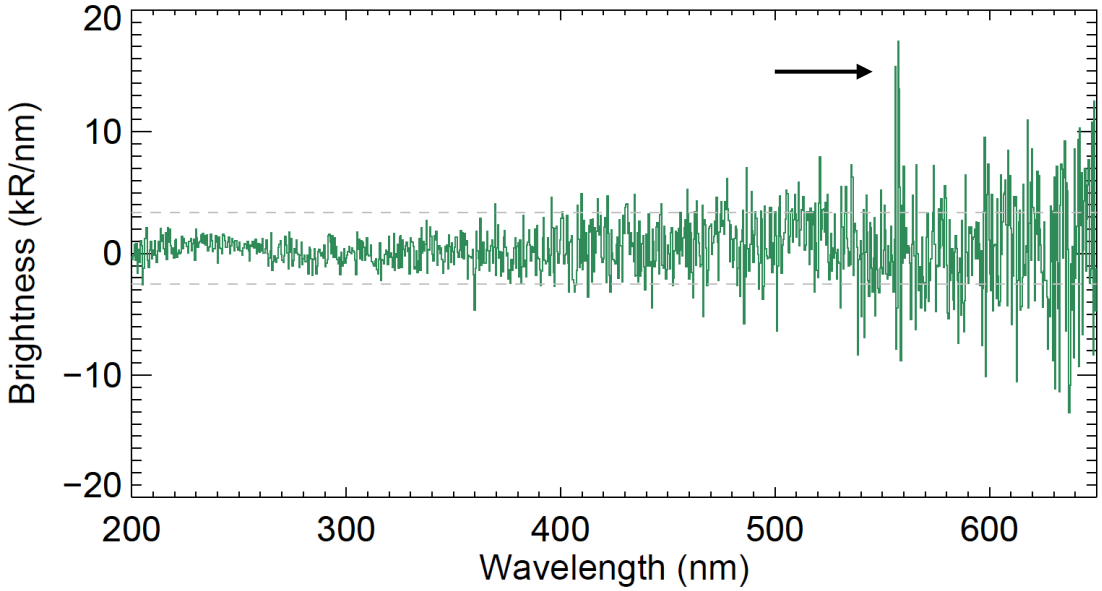

Figure 1: Spectrum of a NOMAD-IUVS limb observation showing the detection of the visible oxygen green line in the Mars aurora. The dashed line indicates the standard deviation of the background noise in this spectral window.

In a second step, all nightside cleaned spectra collected in the crustal field region have been co-added to increase the signal to noise ratio and the probability of detection of a weak auroral signature. Figure 3a shows the result of the addition of 110 nightside spectra collected in this magnetic field region. We clearly note the presence of a peak at 557.7 nm. The mean altitude of the detections is 127.2 km, in good agreement with the 128.2 ± 3.3 km estimated for the OI UV oxygen line by Soret et al. (2021). The line brightness is 5.4 kR, to be compared with the 1-σ noise level of 0.9 kR/nm factor.

Although the CO Cameron, the CO_2^+ UVD and FDB bands are expected to be present, no other auroral feature was observed above the background noise level in the ultraviolet or the visible. Upper limits on the brightness of the Cameron and CO_2^+ UVD bands on the average spectrum are approximately 34 and 2 kR respectively. These values are compatible with the IUVS-MAVEN auroral observations (Soret et al., 2021) of CO Cameron and CO_2^+ UVD emissions concurrent with OI 297.2 nm detections whose mean brightness are 3.7 and 0.5 kR, respectively. Our mean green line brightness of 5.6 kR corresponds to 340 R at 297.2 nm. This value is less than the 420 R of the 1-σ level of the background noise in the UV, which explains why the UV oxygen line cannot be observed in this average spectrum. However, the 340 R value is compatible with the mean OI 297.2 nm brightness of 140 R in the strong B field region given by Soret et al. (2021).

TABLE 1: detections of the 557.7 nm auroral events shown in Figure 2

	Tangent point					**TGO**		
Earth Date (yyyy/mm/dd)	SZA (Deg.)	Local time (hh:mm)	Altitude (km)	Latitude (Deg.)	Longitude (Deg.)	Latitude (Deg.)	Longitude (Deg.)	I(557.7 nm)
2021/06/03[a]	142	21:52	139	-47	22	-52	53	9.1
2021/07/24[b]	151	00:21	130	-53	177	-39	154	10.7
2021/07/25[c]	148	23:59	130	-56	129	-40	108	11.4

[a] Shown in Figure 2a

[b] Shown in Figure 2b

[c] Shown in Figure 1 and Figure 2c

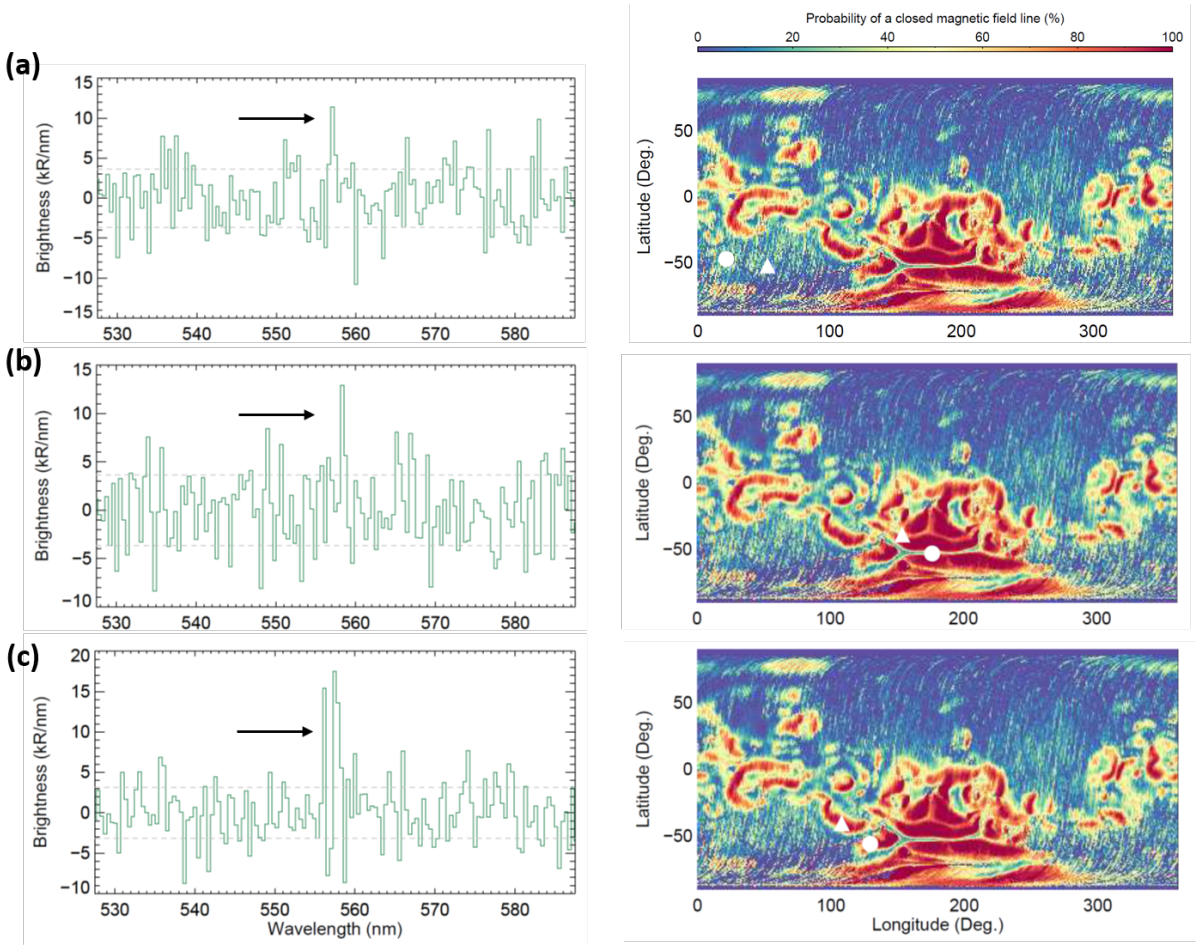

Figure 2: left: (a) nightside individual UVIS spectrum showing a signature at 557.7 nm. The green line brightness is estimated 9.1 kR. (b) 10.7 and (c) 11.4 kR. Right: maps showing the corresponding instantaneous location of the TGO spacecraft (white triangle) and the tangent points (white circle) at ~130 km (see Table 1 for more details). The background colors indicate the probability of open magnetic field line at 400 km (Brain et al., 2007). The tangent points are all located near the limit of open field and closed magnetic lines where ultraviolet auroral events have previously been detected in the ultraviolet .

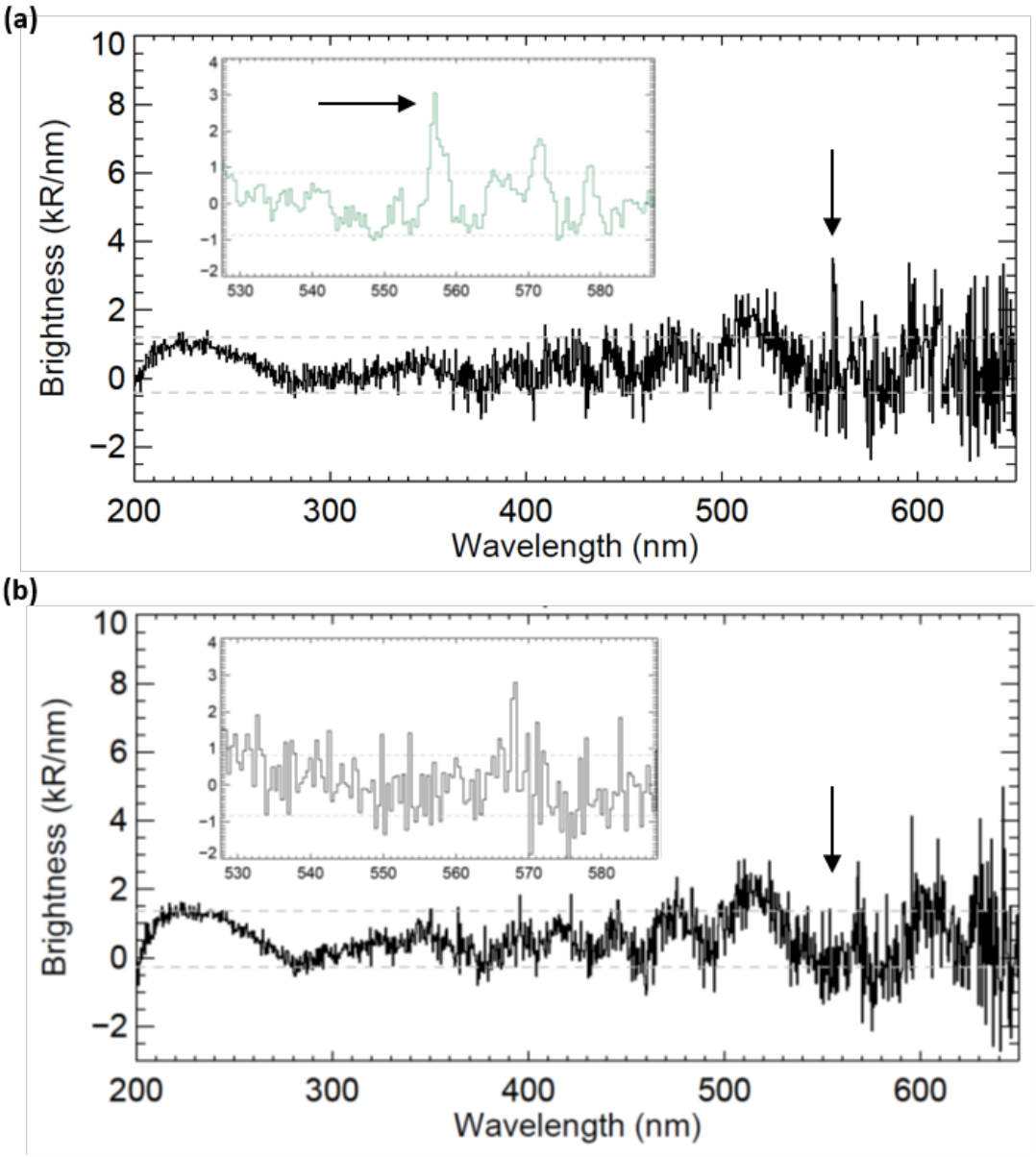

Figure 3: (a) average of 110 nightside UVIS spectra collected in the crustal field region following subtraction of the noise background. The horizontal dotted lines indicate the 1-σ standard deviation of the background noise in the spectral window. No other spectral feature is detected at significant confidence level. (b) average of 220 nightside spectra obtained outside the strong magnetic field region. No spectral feature is identified at 557.7 nm.

The presence of the oxygen green line in the crustal magnetic field region is in agreement with earlier measurements of energetic electron precipitation and discrete ultraviolet auroral events on Mars. The absence of detectable 557.7 nm emission outside this region confirm its links with the magnetic field structures that enhance the particle precipitation as shown in Figure 3b. Our nightglow upper limit of ~0.5 kR is compatible with the lack of detection of the green line from the Mars 3 Soviet probe at a level of 50 rayleighs (Kasnopolsky and Krisko, 1976). During the 15 s of acquisition of one

spectrum, the TGO spacecraft moves by about 60 km. Auroral detections in single 15-s spectra are thus in agreement with the 50-100 km latitudinal extent of the ultraviolet aurora reported by Gérard et al. (2015). Green line detections in individual spectra were only made a few times during the orbital segments of nightside limb tracking observations. The rarity of these occurrences is in conformity with the low frequency of the auroral detections of the OI 297.2 nm line by IUVS (less than 0.2 %) and the limited sensitivity of the UVIS spectrometer at 557.7 nm. The summed spectrum in Figure 3a clearly demonstrates the occasional presence of the auroral green line as it accumulates 110 spectra among which a large fraction does not exhibit the OI signature. Observations of the local time occurrence of the UV aurora has led to the conclusion that auroral events are significantly more frequent before than after local midnight in the B-field sector. Some ambiguity remains concerning the exact location of the auroral emission along the line of sight. The aurora does not necessarily concentrate near the tangent point but may be located at higher altitude along the boresight. It is however notable that the green line detections occur at the same altitude as the OI 297.2 nm emission observed by MAVEN.

The relative intensity of the two $^1S \rightarrow {}^3P$ oxygen lines cannot be directly determined from our auroral spectra where the ultraviolet component is below the UVIS sensitivity threshold. However, our average 557.7 nm brightness of 5.6 kR in the 'strong crustal field region' corresponds to a OI 297.2 nm intensity of 0.34 kR. This is in agreement within a factor of 2 with the average 297.2 nm auroral intensity measured by Soret et al. (2021).

5. MODEL prediction of the green line auroral sources

The $O(^1S)$ metastable state that the radiates the auroral green line emission is mainly excited by collisions of energetic electrons with major constituents:

$$e + CO_2 \rightarrow e + CO + O(^1S) \quad (1)$$

$$e + CO \rightarrow e + C + O(^1S) \quad (2)$$

$$e + O \rightarrow e + O(^1S) \quad (3)$$

We neglect other photochemical sources, such as dissociative recombination of O_2^+ ions whose nightside densities are very low, that make insignificant contribution. Model simulations of the OI 557.7 nm emission produced by these three processes were made

for initial electron energies of 250 and 700 eV using a Monte Carlo electron transport model (Shematovich et al., 2008; Soret et al., 2016). These energies are similar to the average mean electron energy in the discrete aurora (Gérard et al., 2014; Soret et al., 2021). The excitation cross sections for the source processes (1) and (2) were taken from Shirai et al. (2001) and from Itikawa and Ichimura (1990) for (3). For precipitating electrons of 250 eV and 700 eV, the predicted nadir green line brightness is 0.97 kR. and 1.03 kR respectively for a 1 mW m^{-2} electron energy flux. Figure 4 illustrates the production of O(^{1}S) atoms by processes (1) to (3). Electron impact is the main source below 170 km and dominates the contribution to the integrated column production rate. Beyond about 1 keV, the O(^{1}S) production rate steadily drops with increasing energy, similarly to other emissions. We note that, at the peak altitude of the emission and above collisional quenching of O(^{1}S) atoms is negligible. Precipitated electron energy fluxes in excess of 1 mW m^{-2} have been measured in situ concurrently with discrete aurora on several occasions (Gérard et al., 2014; Soret et al., 2021).

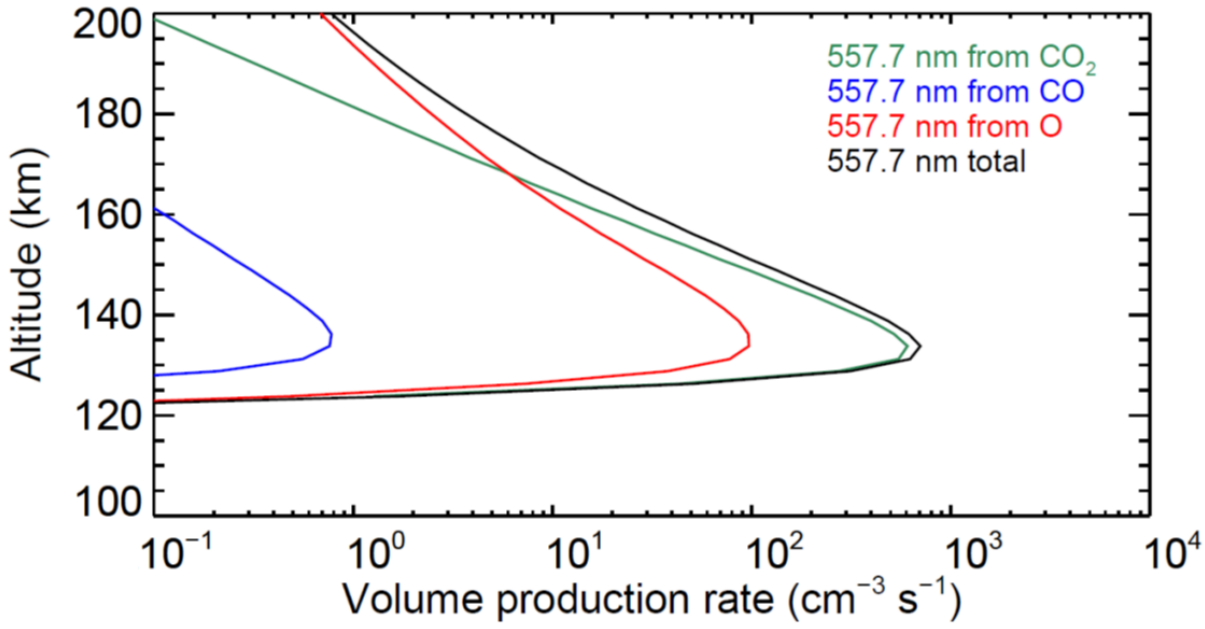

Figure 4: calculated production rate of the O(^{1}S) atoms in the nightside aurora for a precipitation of 700 eV electrons carrying an energy flux of 1 mW m^{-2}. Electron impact on CO_2 dominates the vertical column production.

The mean auroral 557.7 nm brightness of a few kilorayleighs detected from NOMAD is thus fully compatible with the model predictions, considering also that our measurements were made in the limb direction. In addition, they are located in a crustal magnetic field region focusing the precipitation along converging magnetic field lines.

We note that the other emissions are not detected by UVIS, such as the CO_2^+ Fox-Duffendach-Barker(FDB) blue bands that are prominent in laboratory auroral simulators (Lilensten et al., 2015). This lack of other measurable spectral signatures in the UVIS spectra does not imply that they not produced, but molecular bands such as FDB bands are widespread in wavelength and thus do not present peaks above the instrumental background.

6. IMPLICATIONS

An importance consequence of the observations reported here is the possibility to observe the visible aurora with the naked eye by future astronauts in orbit or on the surface. In low-level illumination conditions such as the nightside aurora (scotopic vision) the sensitivity of the human eye peaks near 500 nm. The visibility threshold of the green aurora for human eyes is considered to be on the order of 1 kiloRayleigh (Chamberlain, 2016.) but depends on each individual (Lilensten et al., 2015). It also varies with the morphology of the aurora: narrow localized structures such as the Martian aurora are easier to distinguish than diffuse emissions. Consequently, the oxygen green line is a likely candidate for naked eye observations from orbit or from the Martian surface by potential future astronauts. Measurements of the auroral morphology on the nightside with a visible camera is also an attractive target for upcoming Mars orbiter missions to investigate the detailed morphology, time variations and possible color changes of the aurora.

Acknowledgements. B.H. is research associate and S.A. is postdoctoral researcher of the Belgian Fund for Scientific Research (FNRS). ExoMars is a space mission of the ESA and Roscosmos. The NOMAD experiment is led by the IASB-BIRA, assisted by Co-PI teams from Spain (IAA-CSIC), Italy (INAF-IAPS) and the United Kingdom (The Open University). This project acknowledges funding from BELSPO, with the financial and contractual coordination by the ESA PRODEX Office (PEA grant numbers 4000103401 and 4000121493). M.A.L.-V. and J.-J.L.-M. were supported by grant number PGC2018-101836-B-100 (MCIU/AEI/FEDER, EU) and by the Spanish Science Ministry Centro de Excelencia Severo Ochoa Program under grant number SEV-2017-0709. We also acknowledge support from the UK Space Agency through grant numbers ST/R005761/1, ST/P001262/1, and

ST/S00145X/1ST/R001405/1, 485ST/S00145X/1, ST/R001367/1, ST/P001572/1 and ST/R001502/1 and the Italian Space Agency through grant number 2018-2-HH.0. We thank the ESA TGO team and its project scientist H. Svedhem for his support. The data that support the plots within this paper will be available from BIRA-IASB repository https:// repository.aeronomie/?doi=xxxx or from the corresponding author upon reasonable request.

REFERENCES

Bertaux J.-L. et al., 2005, Discovery of an aurora on Mars, Nature 435, 790–794. https://doi.org/10.1038/nature03603

Brain, D. A., Lillis, R. J., Mitchell, D. L., Halekas, J. S., & Lin, R. P. (2007). Electron pitch angle distributions as indicators of magnetic field topology near Mars. Journal of Geophysical Research, 112, A09201. https://doi.org/10.1029/2007JA012435.

Chamberlain, J. W. (1961). Physics of the Aurora and Airglow, Academic Press.

Deighan, J., Jain, S. K., Chaffin, M. S., Fang, X., Halekas, J. S., Clarke, J. T., ... & Jakosky, B. M. (2018). Discovery of a proton aurora at Mars. Nature Astronomy, 2(10), 802-807.

Gérard J.-C. et al., 2015, Concurrent observations of ultraviolet aurora and energetic electron precipitation with Mars Express, Journal of Geophysical Research, Space Physics, 120, 6749–6765, doi:10.1002/2015JA021150.

Gérard, J. C., Aoki, S., Willame, Y., Gkouvelis, L., Depiesse, C., Thomas, I. R., ... & Mason, J. (2020). Detection of green line emission in the dayside atmosphere of Mars from NOMAD-TGO observations. Nature Astronomy, 124, 5-8. doi:10.1029/2019JA026596.

Gérard, J. C., Aoki, S., Gkouvelis, L., Soret, L., Willame, Y., Thomas, I. R., ... & López-Valverde, M. A. (2021). First observation of the oxygen 630 nm emission in the Martian dayglow. Geophysical Research Letters, 48(8), e2020GL092334

Itikawa, Y. & Ichimura, A. (1990), Cross sections for collisions of electrons and photons with atomic oxygen. J. Phys. Chem. Ref. Data 19, doi:10.1063/1.555857.
Kramida, A., Ralchenko, Y., Reader, J. & NIST ASD Team, 2019, Atomic Spectra Database version 5.7.1 (NIST, 2019). https://physics.nist.gov/asd.

Krasnopolsky, V. A. & Krysko, A. A., (1976). On the night airglow of the Martian atmosphere. XVI, Proceedings of working groups on physical sciences, and symposium and workshop on results from coordinated upper atmosphere measurement programs, Varna,

Bulgaria, Akademie-Verlag GmbH, 1005-1008.

Leblanc F. et al., 2008. Observations of aurorae by SPICAM ultraviolet spectrograph on board Mars Express: Simultaneous ASPERA-3 and MARSIS measurements. JGR, 113, A08311, http://dx.doi.org/10.1029/2008JA013033.

Lilensten, J., Bernard, D., Barthélémy, M., Gronoff, G., Wedlund, C. S. & Opitz, A., 2015, Prediction of blue, red and green aurorae at Mars, Planetary and Space Science, 115, 48-56.

López-Valverde, M. A., Gérard, J.C., González-Galindo, F., Vandaele, A. C., Thomas, I., Korablev, O., ... & Guilbon, S. (2018). Investigations of the Mars Upper Atmosphere with ExoMars Trace Gas Orbiter. Space Science Reviews, 214(1), 29.

Patel, M. R., Antoine, P., Mason, J., Leese, M., Hathi, B., Stevens, A. H., ... & Lewis, S. R. (2017). NOMAD spectrometer on the ExoMars trace gas orbiter mission: part 2—design, manufacturing, and testing of the ultraviolet and visible channel. *Applied optics*, **56**(10), 2771-2782.

Ritter, B., Gérard, J. C., Hubert, B., Rodriguez, L., & Montmessin, F. (2018). Observations of the proton aurora on Mars with SPICAM on board Mars Express. Geophysical Research Letters, 45(2), 612-619. https://doi.org/10.1002/2017GL076235.

Schneider, N. M., Deighan, J. I., Jain, S. K., Stiepen, A., Stewart, A. I. F., Larson, D., ... & Jakosky, B. M. (2015). Discovery of diffuse aurora on Mars. Science, 350(6261).

Schneider, N. M., Jain, S. K., Deighan, J., Nasr, C. R., Brain, D. A., Larson, D., ... & Jakosky, B. M. (2018). Global aurora on Mars during the September 2017 space weather event. Geophysical Research Letters, 45(15), 7391-7398.

Schneider, N. M., Milby, Z., Jain, S. K., Gérard, J. C., Soret, L., Brain, D. A., ... & Jakosky, B. M (2021). Discrete Aurora on Mars: Insights into their distribution and activity from MAVEN/IUVS observations. Journal of Geophysical Research: Space Physics, e2021JA029428.

Shematovich, V. I., Bisikalo, D. V., Gérard, J. C., Cox, C., Bougher, S. W., & Leblanc, F.

(2008). Monte Carlo model of electron transport for the calculation of Mars dayglow emissions. Journal of Geophysical Research: Planets, 113(E2).

Shirai, T., Tabata, T., Tawara, H. (2001). Analytic cross sections for electron collisions with CO, CO_2, and H_2O relevant to edge plasma impurities. Atom. Data Nucl. Data Tables, 79, 143–184.

Soret, L., Gérard, J. C., Libert, L., Shematovich, V. I., Bisikalo, D. V., Stiepen, A., & Bertaux, J. L. (2015). SPICAM observations and modeling of Mars aurorae. Icarus, 264, 398-406.

Soret, L., Gérard, J.-C., Schneider, N., Jain, S., Milby, Z., Ritter, B., et al. (2021). Discrete aurora on Mars: Spectral properties, vertical profiles, and electron energies. Journal of Geophysical Research: Space Physics, 126, e2021JA029495. https://doi.org/10.1029/2021JA029495.

Vandaele, A. C., Neefs, E., Drummond, R., Thomas, I. R., Daerden, F., Lopez-Moreno, J. J., ... & NOMAD Team. (2015). Science objectives and performances of NOMAD, a spectrometer suite for the ExoMars TGO mission. Planetary and Space Science, 119, 233-249.